Disentangling the effects of vegetation and water on the satellite observations of soil organic carbon stocks in western European topsoils

Lixin Lin[1,*], Xixi Liu[2], Yuan Sun[3]

[1]School of Remote Sensing and Geomatics Engineering, Nanjing University of Information Science and Technology, Nanjing, 210044, China
[2]College of Information Science and Engineering, Key Laboratory of Grain Information Processing and Control Ministry of Education, Henan University of Technology, Zhengzhou, 450001, China
[3]College of Surveying and Geo-Informatics, Tongji University, Shanghai, 200092, China

Correspondence to: Lixin Lin (llxshxdhl8@nuist.edu.cn)

Abstract. The performance of models based on satellite observations of soil organic carbon (SOC) stock in European soils is seriously limited by the complexity of natural land surfaces. Therefore, disentangling the SOC stock from other natural land surfaces including vegetation and water bodies has become a rather difficult but necessary task. This study proposed a novel and promising approach intended to resolve this frustrating problem. Based on a series of spectral narrowing, unchanging, and enlarging processes, 23,914,845 sets of SOC models were developed both for vegetation fuzzy disentangling and water fuzzy disentangling. The optimal model was obtained through comparison and was determined as the model that ultimately performed obviously better than the unfuzzified model. This model simulated the per-unit and total SOC stocks in western European topsoils as 99.742 t C ha^{-1} and 9.373 Pg, respectively. In comparison with the results of previous studies, the gaps in the simulated per-unit SOC stocks across the western European countries were considerably narrower (83.673–104.334 t C ha^{-1}). The outstanding model performance and stable simulated per-unit values are the result of disentangling of the vegetation and water cover. This study proposed a valuable reference solution for disentangling the SOC stock from complex natural land cover.

1 Introduction

The amount of carbon stored in Earth's soils is greater than that stored in biomass and the atmosphere (Scharlemann et al., 2014). In recent years, many studies have suggested that environmental degradation and climate change are strongly associated with change of the soil organic carbon (SOC) stock (Crowther et al., 2016; Pries et al., 2017). Therefore, timely observation of SOC stock dynamics is increasingly recognized as of importance. Traditional laboratory-based SOC stock analysis is expensive, laborious, and time consuming. Owing to the advantages of real-time and dynamic tracking, the

method of soil remote sensing that exploits the spectral response of SOC has become a potential alternative for observing SOC stock (Thaler et al., 2019).

The Land Use/Cover Area frame statistical Survey (LUCAS) topsoil database, which is the largest expandable topsoil dataset for the European region, has supported the development of measures intended to protect the soil and environment of

35   the continent (Orgiazzi et al., 2018). The combination of LUCAS and satellite remote sensing provides tremendous potential for timely observation of SOC stock at the European scale (Ward et al., 2020). However, natural land surfaces comprise heterogenous mixtures of vegetation, water, and soil, and the effects of surfaces such as vegetation and water have marked impact on the SOC spectral response, making SOC stock estimation more difficult. Consequently, most previous studies on SOC determination from spectral reflectance focused on optimal soil conditions, i.e., laboratory sieved and air-dried soil

40   samples or small-area bare, dry, and smooth soils (Hutengs et al., 2019; Mueller et al., 2021; Liu et al., 2022). In recent years, some studies have attempted to simulate SOC stock at the European scale. For example, Yigini and Panagos (2016) used the LUCAS topsoil database and multiple linear regression to study the topsoil (0–20 cm) SOC stock in Europe, and their results produced a coefficient of determination (R^2) value of 0.40. Lugato et al. (2014) used the CENTURY agroecosystem model to study the SOC stock in European agricultural topsoil (0–30 cm), and they reported a root mean square error (RMSE) of 52.2

45   and 30.0 t C ha^{-1} for pasture land and permanent cropland, respectively. The low performance of models in such studies has been attributed to many factors but especially complex land cover. Moreover, the areas of vegetation-free and water-free soil in satellite imagery are extremely limited. To adapt to soils with complex surface cover and to apply SOC remote sensing to large geographical regions, the cover of both vegetation and water needs to be disentangled during SOC modeling. Therefore, the focus of this study was the challenging but necessary task of how best to disentangle vegetation and water cover during

50   satellite SOC modeling. Fuzzy deep learning has many advantages when facing uncertainty factors (Tscherko et al., 2007). A study by Lin and Liu (2022) indicated that changing the soil spectral reflectance of soil samples using corresponding soil moisture indexes was helpful for laboratory-based spectroscopic modeling of SOC content. Although their study did not consider that the effects of soil moisture on each spectral band should be different, their adoption of the spectral fuzzy learning approach inspired our research. Hence, our study investigated the issue of "whether the satellite spectral indexes and

55   spectral fuzzy learning (see Materials and methods) are helpful for disentangling the covers of vegetation and water during satellite SOC modeling."

In this study, the two indexes including normalized difference vegetation index (NDVI) and normalized difference water index (NDWI) were used in our spectral fuzzy learning. Based on a series of fuzzy disentangling processes, the SOC model was developed, which produced better performance than the unfuzzified model. Then, this model was used to simulate the

60   SOC stocks for the six western European countries (Belgium, France, Ireland, Luxembourg, Netherlands, and UK (excluding Monaco)).

2 Materials and methods

2.1 Input data

The inputs for SOC modeling included the measured SOC stocks and Landsat-8 images. LUCAS is the largest soil dataset at
65 the European scale (van Deventer et al., 2019) with sampling density of 2×2 km. A total of five subsamples were
composited for each location. Their soil data including SOC, and total contents of sand and clay were measured chemically
after air-drying and sieving through a 2-mm sieve. The measured SOC stocks used in this study were derived using the
LUCAS 2015 database and the following stock calculation function (Huang et al., 2019):

$$SOC \text{ (t C ha}^{-1}) = SOC\% \times Db \text{ (g cm}^{-3}) \times depth \text{ (cm)}$$

(1)

70 where SOC (t C ha^{-1}) and SOC% are the measured SOC stock and the LUCAS 2015 SOC content, respectively, depth (cm)
is the LUCAS sampling depth (20 cm), and Db (g cm^{-3}) represents bulk density data calculated from the bulk density
derived function, as shown in Eq. (2) (Hollis et al., 2012). Hollis et al. (2012) suggested that this bulk density derived
function was useful for calculating the bulk density of European soils. According to Eq. (2), in addition to the LUCAS SOC
content, the LUCAS sand and clay contents were also needed. A total of 754 LUCAS soil samples from the six European
75 countries with sand and clay data were selected.

$$Db \text{ (g cm}^{-3}) = 0.80806 + (0.823844 \times \text{EXP}(-0.27993 \times SOC\%)$$
$$+ (0.0014065 \times Total\ sand\%) - (0.0010299 \times Clay\%)$$

(2)

In recent years, Castaldi (2021) extracted bare soil pixels using threshold values of NDVI of 0–0.35 and normalized burn
ratio 2 (NBR2) of <0.125, and indicated that the bare soil pixel extraction technique was suitable for estimating the topsoil
properties on cropland. Another study by Silvero et al. (2021) used threshold values of NDVI of 0–0.25 and NBR2 of <0.075
80 and suggested that using bare soil pixels was helpful for SOC content mapping in tropical regions. Applying this bare soil
pixel extraction technique to our preprocessing might be of slight benefit for SOC modeling when considering large scales
and complex natural land cover. Therefore, this study used threshold values of NDVI of 0–0.35 and NBR2 of <0.125 to
extract bare soil pixels before SOC modeling. Moreover, organic non-clay (i.e., SOC > 20% and clay < 1%) was eliminated
in this study. Through bare soil pixel extraction and organic non-clay elimination, 300 LUCAS soil samples were selected
85 for our modeling. For these modeling samples, the average SOC stock of Belgium, France, Ireland, Luxembourg, the
Netherlands and UK was 48.697, 103.749, 104.754, 75.927, 73.230, and 92.413 t C ha^{-1}, respectively. Moreover, the SOC
stock of the bare soil pixels was derived using the SOC model, and the SOC stock of the remaining pixels was interpolated
using ordinary kriging, as performed by Yigini and Panagos (2016).

Landsat-8 images of the six western European countries were used as input satellite data. Landsat-8 is the eighth satellite of
90 the Landsat program conducted by the National Aeronautics and Space Administration and the United States Geological
Survey. The spatial resolution and revisit time for Landsat-8 are 30 m and 16 d, respectively. To minimize interference by
clouds, images obtained during March–November 2015 with less cloud cover were (<10 %) were extracted. Spectral bands

1–7 used in this study correspond to the Landsat-8 bands of TM2–4 (visible), TM5 (near-infrared), TM6–7 (shortwave infrared), and TM10 (thermal infrared), respectively. Many studies have indicated that first-order differential transformation

95 is always useful for SOC spectroscopic modeling (Chen et al., 2020). Therefore, this study transformed the 7 original bands into differential bands before SOC modeling, and the 7 original bands and their corresponding 21 differential bands were used as spectral inputs.

2.2 Fuzzy disentangling

Natural land surfaces such as soil, vegetation, and water can affect the spectral reflectance in satellite imagery, and therefore

100 the effects of vegetation and water cover must be considered in SOC stock modeling. If taking vegetation as an example and assuming that two pixels (pixels 1 and 2) correspond to the same SOC stock and different vegetation cover, then one of the following three situations will occur:

(i) If vegetation can increase spectral reflectance, then the pixel with the higher vegetation cover will have higher spectral reflectance and the predicted SOC stock of the two pixels will differ.

105 (ii) If spectral reflectance is independent of vegetation, then the two pixels will have similar spectral reflectance and similar predicted SOC stock.

(iii) If vegetation can decrease spectral reflectance, then their corresponding spectral reflectance and predicted SOC stock should also be different.

If we suppose that we could inverse the spectral reflectance according to the above three situations, the spectral reflectance

110 of satellite imagery could be optimized for the estimation of SOC stock. According to the three situations mentioned in the introduction, the fuzzy formula (f) is designed as follows (Figs. 1 and 2):

$$
\begin{cases}
R_f = R \times f \\
f = p^i \\
i = normalized\ index^j,\ j = 3^{-1}, 2^{-1}, 1, 2\ and\ 3 \\
p = 0.1\ to\ 1\ step\ 0.225,\ and\ 1\ to\ 10\ step\ 2
\end{cases}
\tag{3}
$$

where R_f and R are the spectral reflectance after and before fuzzification, respectively, i is the NDVI/NDWI at different power values (j), and p is the fuzzy parameter. In this equation, p and i are used for the changing pattern and the changing

115 degree, respectively, and i is associated with either vegetation or water. In the interpretation of p: when $p < 1$, R_f will be narrowed—for the situation (i); when $p = 1$, R_f will be unchanged—for the situation (ii); and when $p > 1$, R_f will be enlarged—for the situation (iii). The changing degree depends on the p and i value, tending to increase with increase of the p and i values. Moreover, many previous studies have suggested that NDVI and NDWI can be used for deriving land surface information of vegetation and water, and inspired by the study of Lin and Liu (2022), they used soil moisture indexes to

120 ensure dynamic dewetting. Here, the normalized NDVI and NDWI were used instead of measured vegetation and water values. According to Eq. (3) and Fig. 2, smaller intervals of p and a larger upper boundary of p would produce too many

SOC models during fuzzy disentangling. This study set the lower and upper boundaries of p as 0.1 and 10, respectively, with an interval of 0.225 for the 0.1–1 range and an interval of 2 for the 1–10 range. 0.1 to 1 step 0.225 and 1 to 10 step 2 meant 9 different degrees should be used for each band. Moreover, to enlarge the gaps of satellite spectral indexes and therefore further enhance the changing degrees, five different power values j were also used. The above designs meant that it was necessary to develop a total of $9^7 \times 5 = 23,914,845$ models for the vegetation fuzzy disentangling (Fig. 1). Through comparison, the optimal model from the 23,914,845 models of vegetation fuzzy disentangling could be obtained and its corresponding fuzzified spectra were treated as inputs for water fuzzy disentangling. Similarly, 23,914,845 models were also developed during water fuzzy disentangling, and the optimal model from this step was determined as the ultimate SOC model. The p and j values for the optimal models of the vegetation fuzzy disentangling and the water fuzzy disentangling are shown in the lower part of Fig. 2.

Wadoux et al. (2019) indicated that the random forest (RF) method represents a useful tool for estimating the SOC content of soil samples. Many researchers have suggested that the partial least square (PLS) can reduce the problem of multicollinearity, and thus PLS-RF has been proven a powerful combination tool in spectroscopic modeling (Cardelli et al., 2017; Ballabio et al., 2019; Wang et al., 2019). Therefore, this study used PLS-RF as the regression processing tool, with a principal component number of 6, and decision tree and split node numbers of 10 and 2, respectively. All models developed in this study were validated using the four estimation accuracy indexes of RPD, RMSE, R^2, and MAE (Yigini and Panagos, 2016).
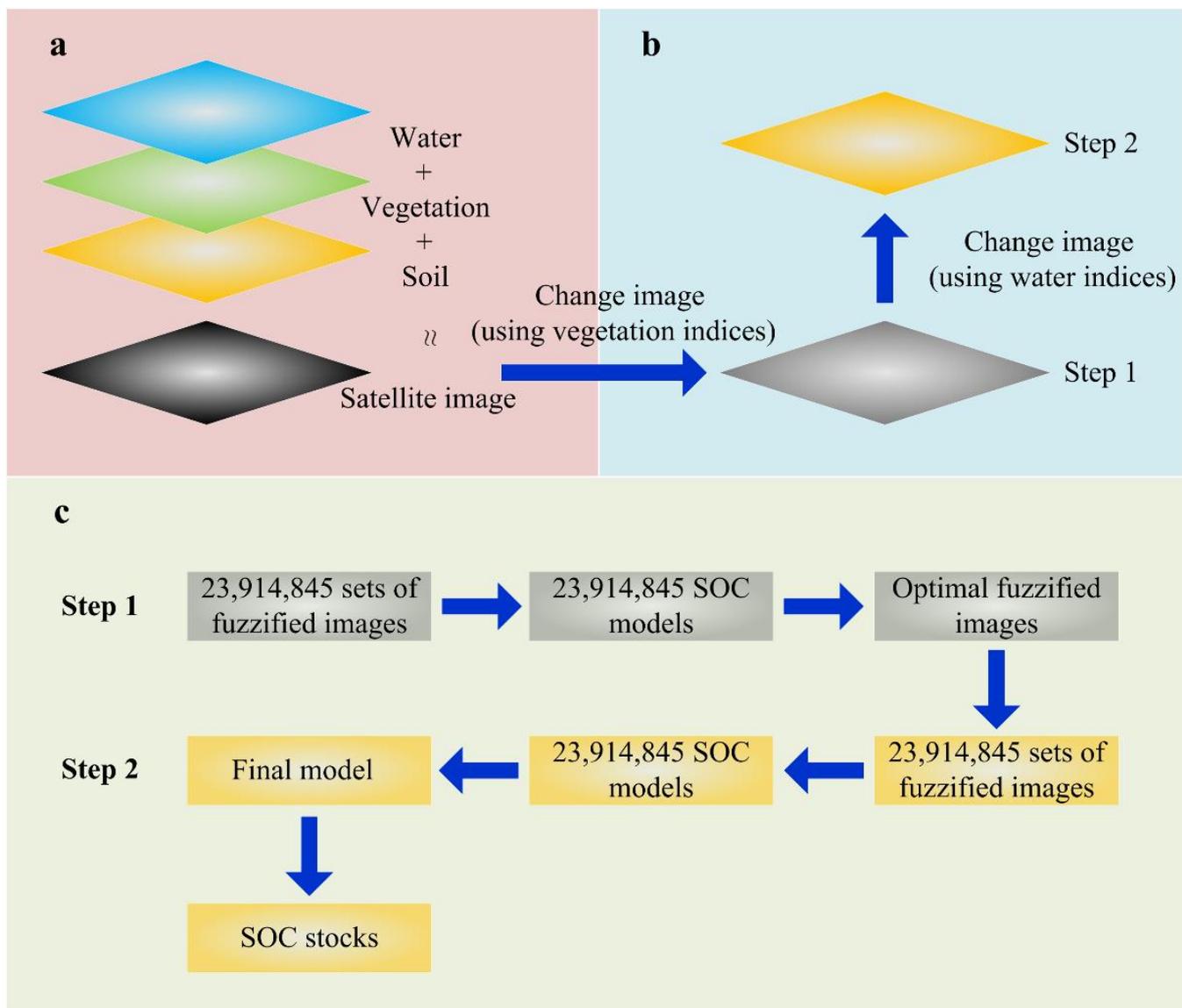
Fig. 1. Diagram of the puzzle and its corresponding solution. (**a**) Earth's natural land surfaces are the mixtures of vegetation, water, soil, etc, this means the other natural land surfaces including vegetation and water must make the satellite remote sensing of soil organic carbon (SOC) stocks difficult. (**b**) The solution works including the vegetation fuzzy disentangling (step 1) and the water fuzzy disentangling (step 2). (**c**) A total of 23,914,845 SOC models were developed during step 1, and based on the fuzzified spectra of the optimal model from these models, 23,914,845 sets of SOC models were also developed during step 2. The optimal model from step 2 was determined as the ultimate SOC model, and its corresponding simulated SOC stocks were also produced.
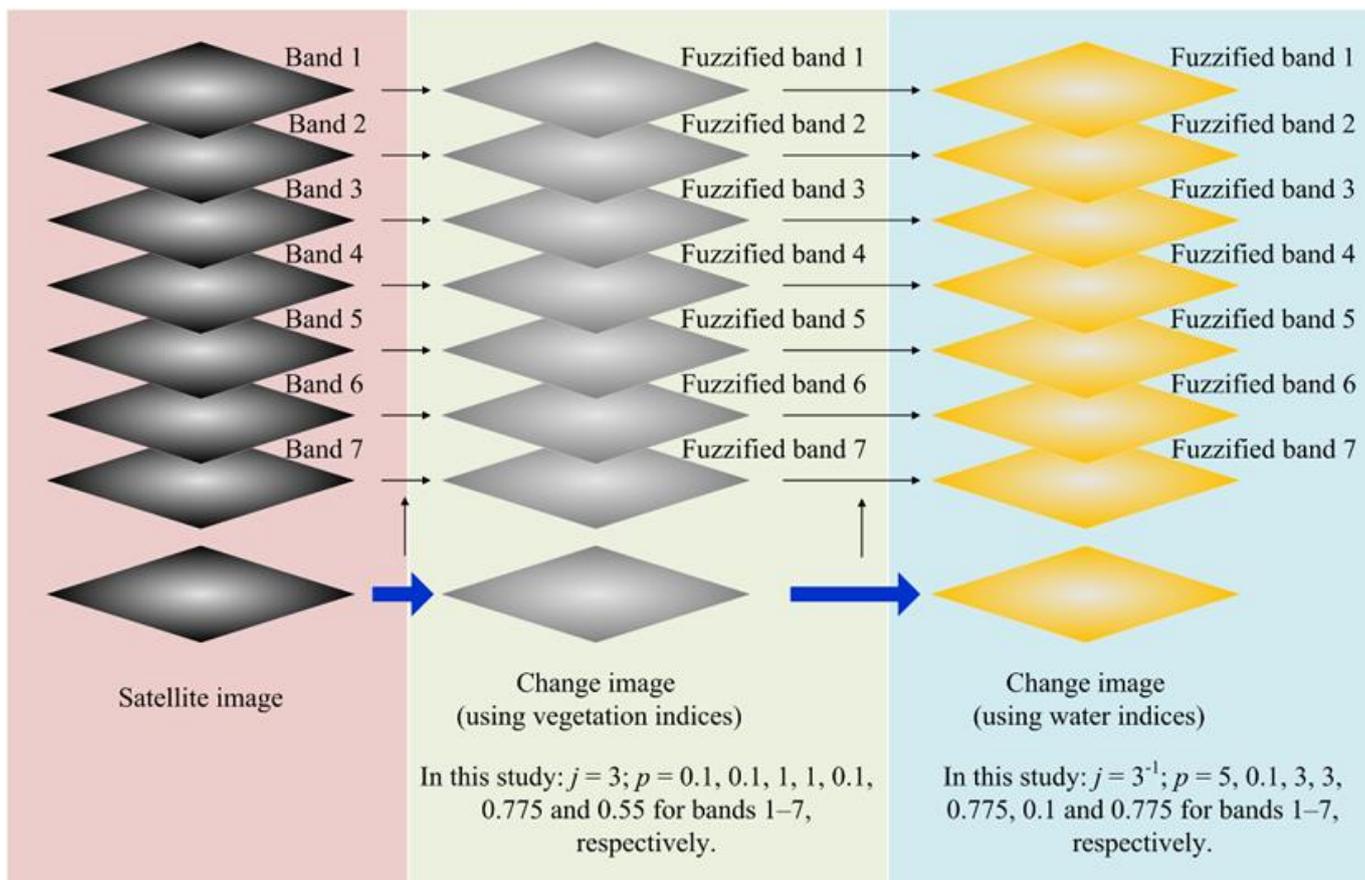
145

Fig. 2. Explanations of the model number. According to Eq. 1, nine different changing patterns (p) should be occurred on each band. In this study, seven Landsat-8 bands were used for modeling. Moreover, five different power values (j) were used to enlarge the gaps of satellite spectral indices. The above designs explained why a total of $9^7 \times 5 = 23{,}914{,}845$ models needed to be developed both for the vegetation fuzzy disentangling and the water fuzzy disentangling. p and j values for the optimal models from the vegetation fuzzy

150 disentangling and water fuzzy disentangling were obtained through model comparisons.

3 Results and discussion

3.1 Simulated SOC stock in western Europe

The simulated per-unit topsoil (0–20 cm) SOC stock in each of the six western European countries is shown in Fig. 3a. It can be seen that the country with the highest simulated per-unit SOC stock was France (104.334 t C ha^{-1}), followed by Ireland

155 and the UK with a value of 94.646 and 94.335 t C ha^{-1}, respectively. The country with the lowest simulated per-unit SOC stock was the Netherlands, with a value of 83.673 t C ha^{-1}. It can be seen from Fig. 3b that France had the highest simulated total SOC stock (5.769 Pg) and that Luxembourg had the lowest value (0.024 Pg). The per-unit SOC stock for all six countries was simulated as 99.742 t C ha^{-1}, corresponding to a total SOC stock of 9.373 Pg. Table 1 presents comparison of European SOC stock as determined by the two studies mentioned in the introduction (the simulated per-unit SOC stocks of

160 Yigini and Panagos (2016) were calculated using the simulated total SOC stock in their published paper). Comparison with

Yigini and Panagos (2016) indicates that the per-unit and total stock SOC stocks for all six countries in our work were slightly higher (i.e., 99.742 t C ha^{-1} versus 94.18 t C ha^{-1} and 9.373 Pg versus 8.85 Pg). Interestingly, our simulated per-unit results across the six countries had obviously narrower gaps (i.e., 83.673–104.334 t C ha^{-1} versus 58.45–154.90 t C ha^{-1}). The results from Lugato et al. (2014) indicate that their simulated per-unit SOC stocks in the Mediterranean regions and

165   northeastern regions tended to be < 40 and 80–250 40 t C ha^{-1}, respectively. Many hotspot regions including Ireland, the Netherlands, the UK, and Finland produced extremely high simulated per-unit SOC stocks with values of > 250 t C ha^{-1}. Although their study only covered agricultural topsoil (0–30 cm), the comparison results further indicate the narrower simulated per-unit SOC gaps of our work. This is an interesting finding and deserves to be investigated further in the future. The simulated SOC stock distribution and the digital elevation model (DEM) of the six countries are shown in Fig. 3c–d.

170   Over the entire western European region, the simulated SOC stocks tended to increase as the DEM value increased. Taking France and the UK as examples, the central south, southeast, and south of France, the west of England, and most regions of Scotland and Wales had obviously high levels of simulated SOC stock. These high-elevation regions include the Central Plateau, Alps, and Pyrenees of France, the Pennine Hills of England, the Highlands and Southern Uplands of Scotland, and the Cambrian Mountains of Wales. It can also be seen from Fig. 4c that most regions of England and the Netherlands and the

175   northwest of France had relatively low simulated SOC stocks, and Fig. 4d shows that these regions are generally low-lying areas. Bojko et al. (2017) indicated that the distribution of SOC is associated with elevation. Prietzel and Christophel (2014) studied the forest soils in the German Alps and found that soils at high-elevation sites with low air temperature and high precipitation had obviously high SOC stock. The finding of our study of a general trend of high-elevation regions having high per-unit topsoil SOC stock supports the previous findings. Regions with elevation of > 1000 m were not sampled in the

180   LUCAS campaigns; instead, the SOC stock was derived using the SOC model and satellite imagery, as in the study by Yigini and Panagos (2016). Therefore, this is an area that deserves further investigation in future work.
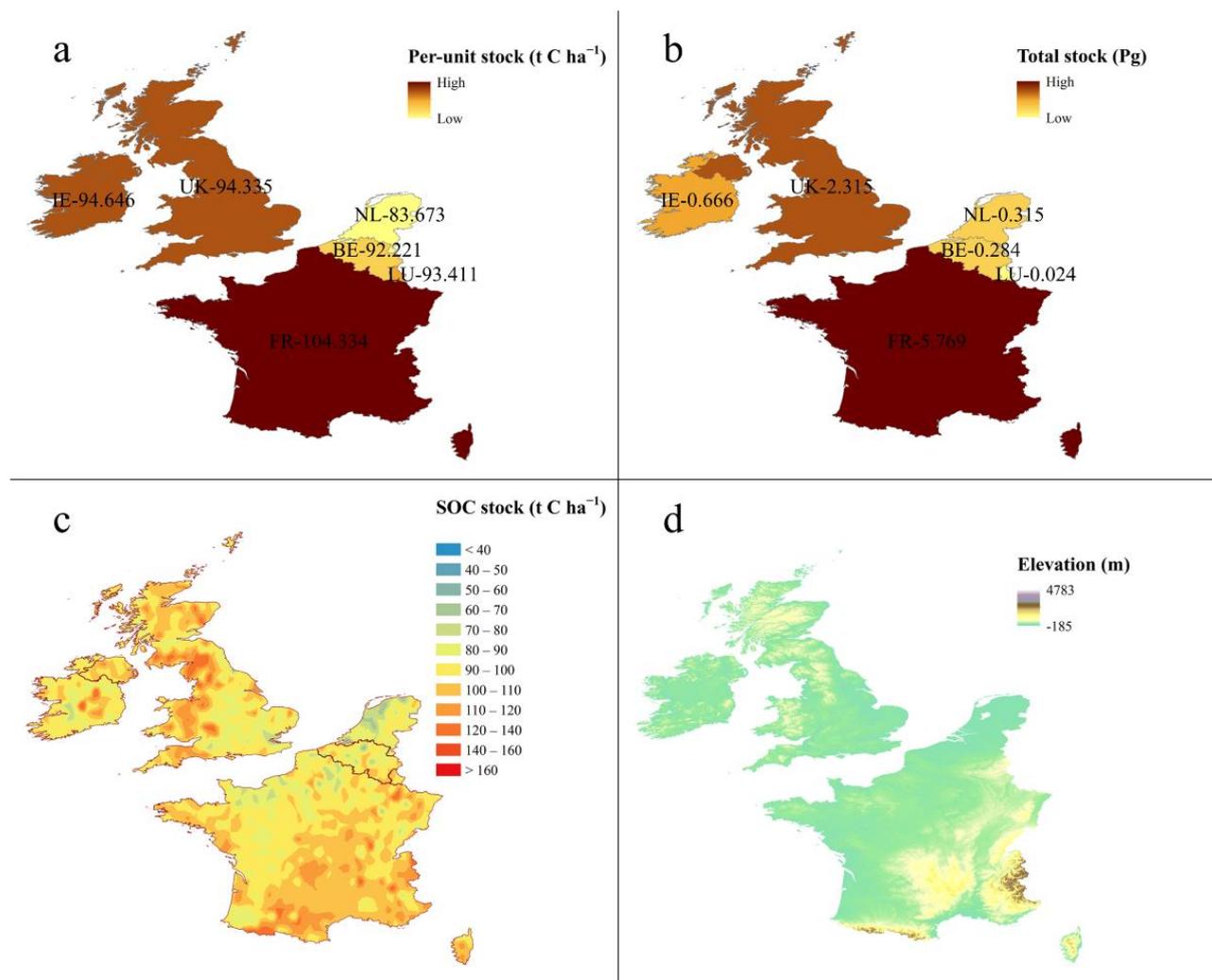
Fig. 3. Simulated soil organic carbon (SOC) stocks. Simulated (**a**) per-unit and (**b**) total topsoil (0–20 cm) SOC stocks in the six western European countries (Belgium, France, Ireland, Luxembourg, Netherlands and United Kingdom (UK)). (**c**) Simulated SOC stock distributions and (**d**) digital elevation model (DEM) in the six countries.

Table 1 Simulated soil organic carbon (SOC) stocks in this work and some previous studies

This work			Yigini and Panagos (2016)			Lugato et al. (2014)	
Region	Per-unit	Total	Region	Per-unit	Total	Region	Per-unit
Belgium	92.221	0.284	Belgium	58.45	0.18	Mediterranean regions	Tend to < 40
France	104.334	5.769	France	68.90	3.81	North-eastern Europe	80–250
Ireland	94.646	0.666	Ireland	154.90	1.09	Hotspot situations	> 250
Luxembourg	93.411	0.024	Luxembourg	77.84	0.02	Whole Europe	82.4
Netherlands	83.673	0.315	Netherlands	71.72	0.27	Netherlands	100.1
UK	94.335	2.315	UK	141.81	3.48		
Six countries	99.742	9.373	Six countries	94.18	8.85		

The study by Lugato et al. (2014) refers to the agricultural topsoils (0–30 cm), and the hotspot regions with the simulated per-unit SOC stocks > 250 t C ha^{-1} including Ireland, Netherlands, UK and Finland; This work and the study by Yigini and Panagos (2016) refer to all the land uses (0–20 cm).

3.2 Model performance

The first phase of this work was to develop the SOC model. Based on spectral narrowing, unchanging, and enlarging processes with different degrees, a total of 23,914,845 SOC models were developed during the water fuzzy disentangling. A selection of the models with a ratio of performance to deviation (RPD) of >1.3 is shown in Fig. 4a–d. It can be seen that the RMSE, R^2, and mean absolute error (MAE) of these models varied markedly (i.e., RMSE: 20.054–26.527 t C ha^{-1}, R^2: 0.534–0.708, MAE: 17.078–21.893 t C ha^{-1}). Through comparison, the optimal model with values of RPD of 1.500, RMSE of 20.054 t C ha^{-1}, R^2 of 0.708, and MAE of 17.078 t C ha^{-1} was obtained and determined as the ultimate SOC model (Fig. 4e). Moreover, the spectral inputs of the water fuzzy disentangling were obtained from the vegetation fuzzy disentangling, i.e., the corresponding fuzzified spectra of the optimal model from the 23,914,845 models obtained during the vegetation fuzzy disentangling. This model had values of RPD of 1.269, RMSE of 22.042 t C ha^{-1}, R^2 of 0.669, and MAE of 17.379 t C ha^{-1}.

The SOC model developed based on unfuzzified spectra is shown in Fig. 4f. This model had values of RPD of 0.822, RMSE of 32.598 t C ha^{-1}, R^2 of 0.282, and MAE of 26.477 t C ha^{-1}, indicating comparable model performance with that reported by the previous studies at the European scale. For example, De Brogniez et al. (2015) and Meersmans et al. (2008) used generalized additive models to study the topsoil SOC content of European countries, and the R^2 value of each of their models was 0.29 and 0.36, respectively. Similarly, Bell and Worrall (2009) mapped SOC content at the regional scale and realized a value of R^2 of 0.48. As already mentioned in the introduction, Yigini and Panagos (2016) investigated SOC stock in Europe and found reported an R^2 value of 0.40. They attributed the low performance of their model to many factors but especially to the effect of complex natural land cover. It can be seen from Fig. 4e that the SOC model with fuzzy disentangling provided better RPD, RMSE, R^2 and MAE values, and that its samples were closer to the 1:1 line than the samples of the unfuzzified model. The evident better performance of the model with fuzzy disentangling must be the result of the fuzzy disentangling processes. The comparison results both support the previous assertion that complex natural land cover can substantially increase the difficulty of satellite-based modeling of SOC stock and demonstrate the potential of the fuzzy disentangling approach.
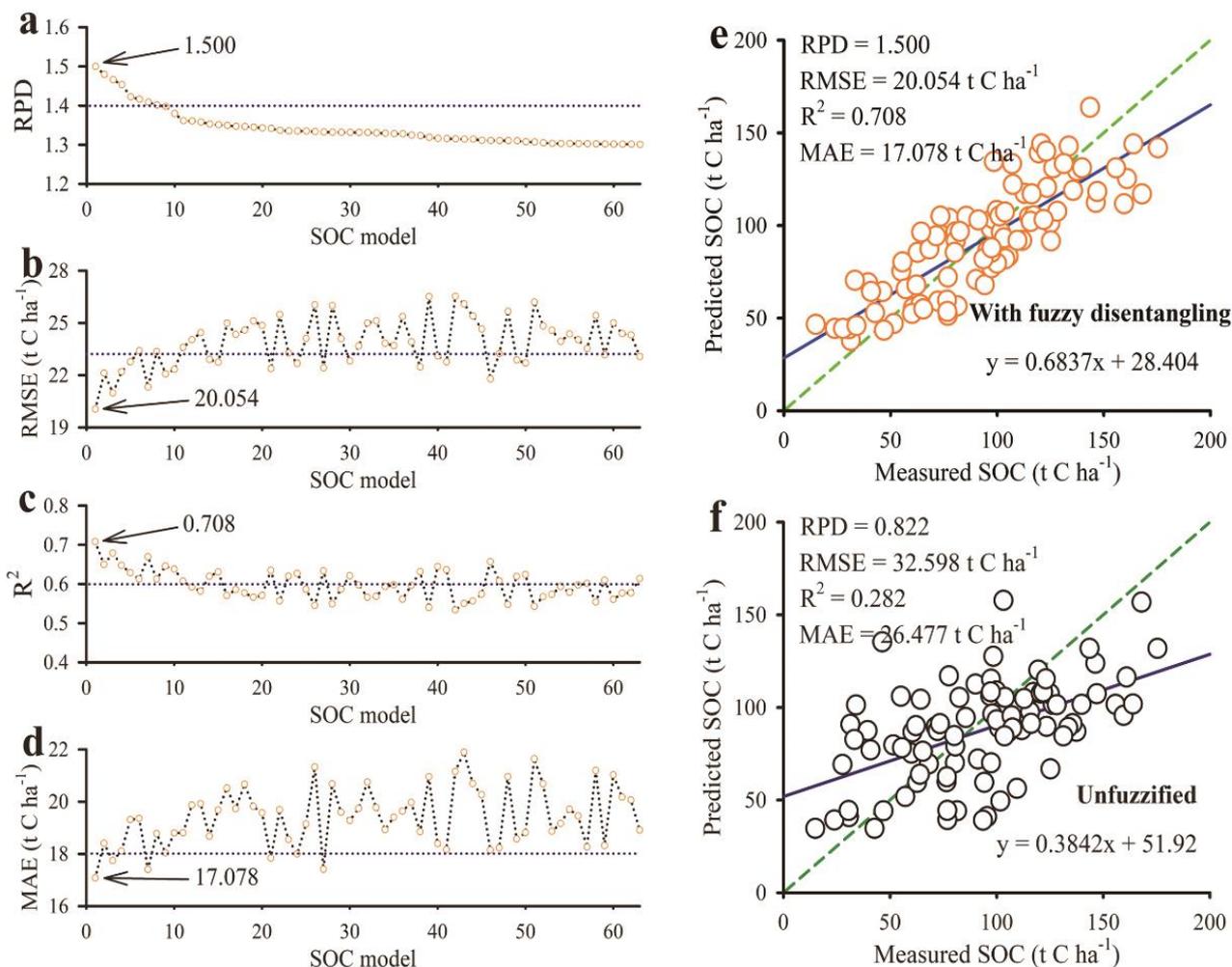
Fig. 4. Model performance. (**a**) Ratio of performance to deviation (RPD), (**b**) root mean squared error (RMSE), (**c**) R-squared (R^2) and (**d**) mean absolute error (MAE) of the SOC models during fuzzy disentangling. Validation results of (**e**) the SOC model with fuzzy disentangling versus (**f**) the model without fuzzy disentangling.

4 Conclusions

This study attempted to disentangle the SOC stock from complex vegetation and water cover, and the two indexes including NDVI and NDWI were used. Based on the processes of vegetation fuzzy disentangling and water fuzzy disentangling, the SOC model gave better results than the unfuzzified model because of its fuzzy disentangling processes. This model then was used to simulate the SOC stocks in western European topsoils. This study proposed a potential solution for disentangling SOC stock from complex vegetation and water cover, represents a valuable reference for addressing the difficulties of satellite-based observation of continental SOC stock.

Competing interests

The contact author has declared that none of the authors has any competing interests.

Acknowledgments

The research was funded by the National Natural Science Foundation of China (grant no. 42107491). We also thank the European Soil Data Centre, European Space Agency, National Aeronautics and Space Administration, and United States Geological Survey for supporting the research data. We thank James Buxton, MSc, from Liwen Bianji (Edanz) (www.liwenbianji.cn/), for editing the English text of a draft of this manuscript.

References

Ballabio, C., Lugato, E., Fernandez-Ugalde, O., Orgiazzi, A., Jones, A., Borrelli, P., Montanarella, L., Panagos, P.: Mapping LUCAS topsoil chemical properties at European scale using Gaussian process regression, Geoderma, 355, 1–14, doi: 10.1016/j.geoderma.2019.113912, 2019.

Bell, M.J., Worrall, F.: Estimating a region's soil organic carbon baseline: the undervalued role of land-management, Geoderma, 152, 74–84, doi: 10.1016/j.geoderma.2009.05.020, 2009.

Bojko, O., Kabala, C., Mendyk, L., Markiewicz, M., Pagacz-Kostrzewa, M., Glina, B.: Labile and stabile soil organic carbon fractions in surface horizons of mountain soils-relationships with vegetation and altitude, J. MT. Sci, 14, 2391–2405, 2017.

Cardelli, V., Weindorf, D.C., Chakraborty, S., Li, B., De Feudis, M., Cocco, S., Agnelli, A., Choudhury, A., Ray, D.P., Corti, G.: Non-saturated soil organic horizon characterization via advanced proximal sensors, Geoderma, 288, 130–142, doi: 10.1016/j.geoderma.2016.10.036, 2017.

Castaldi, F.: Sentinel-2 and Landsat-8 Multi-Temporal Series to Estimate Topsoil Properties on Croplands, Remote Sen, 13, 1–15, doi: 10.3390/rs13173345, 2021.

Chen, Y., Li, Y.Q., Wang, X.Y., Wan, J.L., Gong, X.W., Niu, Y.Y., Liu, J.: Estimating soil organic carbon density in Northern China's agro-pastoral ecotone using vis-NIR spectroscopy, J. Soil. Sediment, 20, 3698–3711, doi: 10.1007/s11368-020-02668-2, 2020.

Crowther, T.W., et al.: Quantifying global soil carbon losses in response to warming, Nature, 540, 104–108, 2016.

De Brogniez, D., Ballabio, C., Stevens, A., Jones, R.J.A., Montanarella, L., van Wesemael, B.: A map of the topsoil organic carbon content of Europe generated by a generalized additive model, Eur. J. Soil Sci., 66, 121–134, doi: 10.1111/ejss.12193, 2015.

Hollis, J.M., Hannam, J., Bellamy, P.H.: Empirically-derived pedotransfer functions for predicting bulk density in European soils, Eur. J. Soil Sci., 63, 96–109, 2012.

Huang, J.Y., Hartemink, A.E., Zhang, Y.K.: Climate and Land-Use Change Effects on Soil Carbon Stocks over 150 Years in
255 Wisconsin, USA, Remote Sen, 11, 1–20, doi: 10.3390/rs11121504, 2019.

Hutengs, C., Seidel, M., Oertel, F., Ludwig, B., Vohland, M.: In situ and laboratory soil spectroscopy with portable visible-to-near-infrared and mid-infrared instruments for the assessment of organic carbon in soils, Geoderma, 355, 1–11, doi: 10.1016/j.geoderma.2019.113900, 2019.

Lin, L.X., Liu, X.X.: Soil-moisture-index spectrum reconstruction improves partial least squares regression of spectral
260 analysis of soil organic carbon, Precis. Agric., 1–13, doi: 10.1007/s11119-022-09905-3, 2022.

Liu, J., Zhang, D.X., Yang, L., Ma, Y.X., Cui, T., He, X.T., Du, Z.H.: Developing a generalized vis-NIR prediction model of soil moisture content using external parameter orthogonalization to reduce the effect of soil type, Geoderma, 419, 1–9, 2022.

Lugato, E., Panagos, P., Bampa, F., Jones, A., Montanarella, L.: A new baseline of organic carbon stock in European agricultural soils using a modelling approach, Global Change Biol., 20, 313–326, doi: 10.1111/gcb.12292, 2014.

265 Meersmans, J., De Ridder, F., Canters, F., De Baets, S., Van Molle, M.: A multiple regression approach to assess the spatial distribution of soil organic carbon (SOC) at the regional scale (Flanders, Belgium), Geoderma, 143, 1–13, doi: 10.1016/j.geoderma.2007.08.025, 2008.

Mueller, C.W., Steffens, M., Buddenbaum, H.: Permafrost soil complexity evaluated by laboratory imaging Vis-NIR spectroscopy. Eur. J. Soil Sci., 72, 114–119 , 2021.

270 Orgiazzi, A., Ballabio, C., Panagos, P., Jones, A., Fernández-Ugalde, O.: LUCAS Soil, the largest expandable soil dataset for Europe: A review, Eur. J. Soil Sci., 69, 140–153, doi: 10.1111/ejss.12499, 2018.

Pries, C.E.H., Castanha, C., Porras, R.C., Torn, M.S.: The whole-soil carbon flux in response to warming, Science, 355, 1420–1422, 2017.

Prietzel, J., Christophel, D.: Organic carbon stocks in forest soils of the German Alps, Geoderma, 221, 28–39, doi:
275 10.1016/j.geoderma.2014.01.021, 2014.

Scharlemann, J.P.W., Tanner, E.V.J., Hiederer, R., Kapos, V.: Global soil carbon understanding and managing the largest terrestrial carbon pool, Carbon Manag., 5, 81–91, 2014.

Silvero, N.E.Q., Dematte, J.A.M., Amorim, M.T.A., dos Santos, N.V., Rizzo, R., Safanelli, J.L., Poppiel, R.R., Mendes, W.D., Bonfatti, B.R.: Soil variability and quantification based on Sentinel-2 and Landsat-8 bare soil images: A comparison,
280 Remote Sens. Environ, 252, 1–19, 2021.

Thaler, E.A., Larsen, I.J., Yu, Q.: A New Index for Remote Sensing of Soil Organic Carbon Based Solely on Visible Wavelengths, Soil Sci. Soc. Am. J., 83, 1443–1450, doi: 10.2136/sssaj2018.09.0318, 2019.

Tscherko, D., Kandeler, E., Bardossy, A.: Fuzzy classification of microbial biomass and enzyme activities in grassland soils, Soil Biol. Biochem, 39, 1799–1808, 2007.

285 van Deventer, H., Cho, M.A., Mutanga, O.: Multi-season RapidEye imagery improves the classification of wetland and dryland communities in a subtropical coastal region, ISPRS J. Photogramm, 157, 171–187, doi: 10.1016/j.isprsjprs.2019.09.007, 2019.

Wang, J.J., Zareef, M., He, P.H., Sun, H., Chen, Q.S., Li, H.H., Ouyang, Q., Guo, Z.M., Zhang, Z.Z., Xu, D.L.: Evaluation of matcha tea quality index using portable NIR spectroscopy coupled with chemometric algorithms, J. Sci. Food Agr., 99,
290   5019–5027, doi: info:doi/10.1002/jsfa.9743, 2019.

Ward, K.J., Chabrillat, S., Brell, M., Castaldi, F., Spengler, D., Foerster, S.: Mapping Soil Organic Carbon for Airborne and Simulated EnMAP Imagery Using the LUCAS Soil Database and a Local PLSR, Remote Sens., 12, 1–20, doi: 10.3390/rs12203451, 2020.

Wadoux, A.M.J.C., Brus, D.J., Heuvelink, G.B.M., 2019. Sampling design optimization for soil mapping with random forest,
295   Geoderma, 355, 1–11.

Yigini, Y., Panagos, P. Assessment of soil organic carbon stocks under future climate and land cover changes in Europe, Sci. Total Environ., 557, 838–850, doi: 10.1016/j.scitotenv.2016.03.085, 2016.